



## Low-Temperature Dynamics of Water Confined in Unidirectional Hydrophilic Zeolite Nanopores

Maria Rescigno, Matilde Luciola, Frederico G Alabarse, Umbertoluca Ranieri, Bernhard Frick, Benoit Coasne, Livia Bove

### ► To cite this version:

Maria Rescigno, Matilde Luciola, Frederico G Alabarse, Umbertoluca Ranieri, Bernhard Frick, et al.. Low-Temperature Dynamics of Water Confined in Unidirectional Hydrophilic Zeolite Nanopores. Journal of Physical Chemistry B, 2023, 127 (20), pp.4570-4576. 10.1021/acs.jpcb.3c00681 . hal-04236137

**HAL Id: hal-04236137**

**<https://cnrs.hal.science/hal-04236137>**

Submitted on 10 Oct 2023

**HAL** is a multi-disciplinary open access archive for the deposit and dissemination of scientific research documents, whether they are published or not. The documents may come from teaching and research institutions in France or abroad, or from public or private research centers.

L'archive ouverte pluridisciplinaire **HAL**, est destinée au dépôt et à la diffusion de documents scientifiques de niveau recherche, publiés ou non, émanant des établissements d'enseignement et de recherche français ou étrangers, des laboratoires publics ou privés.

# Low temperature dynamics of water confined in hydrophilic zeolite nanopores


*Matilde Luciolì<sup>£</sup>, Maria Rescigno<sup>£</sup>, Frederico G. Alabarse<sup>§</sup>, Umbertoluca Ranieri<sup>£</sup>, Bernhard*

*Frick , Benoit Coasne , Livia E. Bove <sup>†£\*</sup>*

<sup>£</sup> Dipartimento di Fisica, Università di Roma La Sapienza, Roma, Italy.

<sup>†</sup> Sorbonne Université, UMR CNRS 7590, Institut de Minéralogie, de Physique des Matériaux et de Cosmochimie (IMPMC), Paris, France.

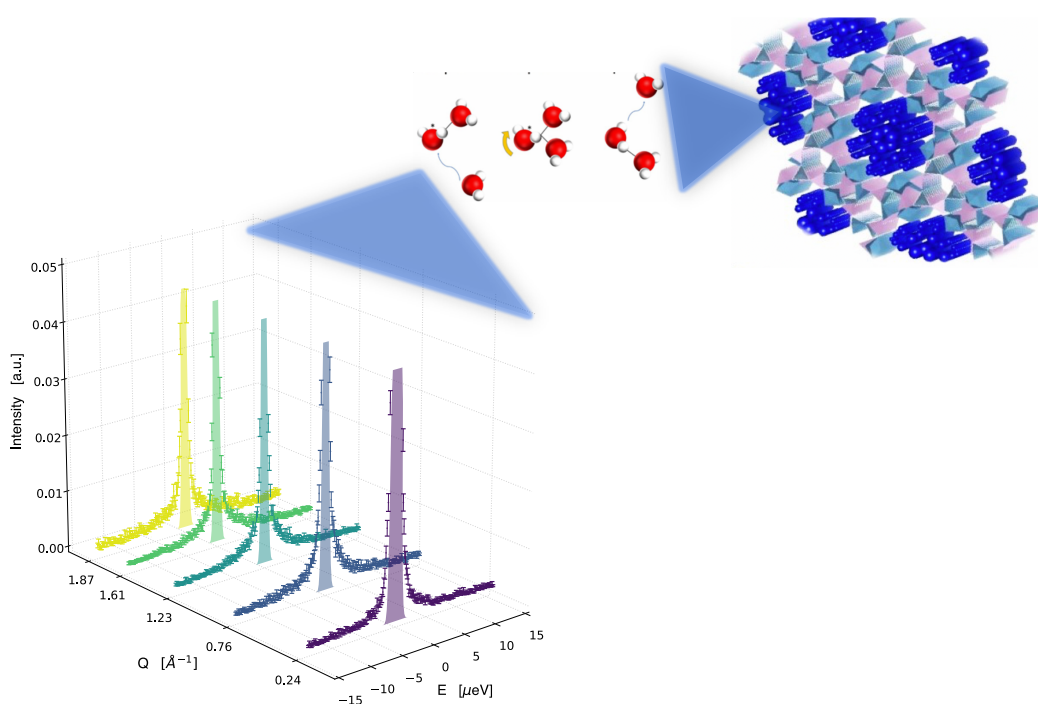
<sup>§</sup> Elettra Sincrotrone Trieste, Basovizza, Trieste, Italy.

 Institut Laue-Langevin, Grenoble Cedex 9, France.

 Université Grenoble Alpes, CNRS, LIPhy, 38000 Grenoble, France.

## ABSTRACT

*The dynamical properties of water molecules confined in the hydrophilic nanopores of  $\text{AlPO}_4\text{-54}$  zeolite investigated with Quasi-Elastic Neutron scattering as a function of temperature down to 2 K. Water molecular diffusion into the pore is measured down to 258 K. Diffusion follows a jump mechanism with a jump distance increasing with temperature and an activation energy of  $E_a = (20.8 \pm 2.8)$  kJ/mol, in agreement with previous studies on similar confining media. Water rotational diffusion is instead measured down to temperatures (118 K) well below the water glass transition. The rotational time scale shows a non-Arrhenius behavior down to the freezing of water diffusion, while it has a feeble temperature dependence below. This fast molecular re-orientation (fractions of nanoseconds) is believed to take place in the dense, highly disordered amorphous water present in the pore center, therefore indicating its plastic amorphous nature.*



## 1. Introduction

Zeolites are crystalline microporous materials (pore size < 2 nm) constituted primarily by  $\text{SiO}_4$  and  $\text{AlO}_4$  corner-sharing tetrahedral building units that form a three-dimensional structure. These relatively rigid anionic frameworks contain exchangeable cations and generally removable and replaceable guest molecules such as water and organic compounds. These porous materials are known as “molecular sieves” because of their high and tailorable acidity and their specific pore structures with channels and cavities of molecular dimensions which allow shape-selective conversions of organic molecules. The void space within the crystal allows indeed zeolites to discriminate molecules based on their size or geometric shape. One of the biggest everyday uses for zeolites is indeed as water softeners and water filters. Zeolites have also been employed in a wide range of industrial applications such as adsorption/separation, ion-exchange processes and also as catalysts in the processes of oil refining and fine chemical synthesis [3-5].

$\text{AlPO}_4\text{-54}$  belongs to the family of  $\text{AlPO}_4\text{-n}$  zeolites, the first zeolites synthesized without silica. This zeolite is of particular interest as it exhibits 1D pores along the  $c$  direction of the crystal (hexagonal VFI structure, space group  $P6_3$ ,  $a=18.9678(13)$  Å and  $c=8.0997(4)$  Å,  $\text{Al}_{18}\text{P}_{18}\text{O}_{72}\cdot x\text{H}_2\text{O}$ ) [3] with a diameter of 12.7 Å, i.e. it has among the largest pores known for zeolites and aluminophosphates. The zeolite framework is built up of 4, 6 and 18-membered rings of alternating  $\text{AlO}_6$ ,  $\text{AlO}_4$  and  $\text{PO}_4$  polyhedra. When water is inserted in  $\text{AlPO}_4\text{-54}$  pores, one-third of the aluminium welcome two  $\text{H}_2\text{O}$  molecules in their coordination sphere, this “structural water” is strongly linked to the zeolite structure and can be extracted only under secondary vacuum treatment [6,7]. Remaining water is inserted in the zeolite pore and forms a disordered hydrogen-bonded network in the centre of the pore at ambient pressure and temperature conditions. When the temperature is lowered, pore water crystallization is prevented due to the

high degree of confinement and the water network differentiates into two distinct networks whose local arrangement and dynamical behavior depend on the proximity with the pore walls [8]. Upon cooling below ice homogeneous nucleation temperature, water close to the zeolite pore surface assumes a highly ordered local arrangement induced by the pore wall, with a more defined site occupancy and lower density with respect to bulk water. In contrast, under the same conditions, water in the pore core shows a denser, more disordered, and orientationally distorted glassy arrangement [8].

While the role of the chemistry of the pore surface on water structuring is rather well understood, its effects on water dynamics have been poorly investigated experimentally. Yet, these effects are fundamental for the potential application of this material as nanosieve for water filtration and purification .

Since  $\text{AlPO}_4\text{-54}$  has both hydrophobic and hydrophilic groups, it is expected that water flow would be larger for  $\text{AlPO}_4\text{-54}$  than the flux observed in pure alumina pores. However, molecular dynamics simulations for this system [9] did not observe any super-flow phenomenon, such as the one observed in carbon nanotubes where the single-line arrangement of the water molecules into the pores gives rise to a flow orders of magnitude faster than in the bulk [10,11]. Contrary to the case of carbon and alumina nanotubes, the surface of the  $\text{AlPO}_4\text{-54}$  pore is not « atomically smooth » [7], and the structural organization of the inner water molecules is much denser and disordered [8]. How all this affects the water dynamics is the object of the present study.

Here we report high-resolution quasi-elastic neutron scattering (QENS) experiments probing water diffusive and orientational dynamics into the hydrophilic nanopores of fully hydrated  $\text{AlPO}_4\text{-54}$  from room temperature down to 2 K. We observe that nanoconfined water molecular diffusion at room

temperature is a factor three slower than in bulk water, as expected for water in hard confinement, and can be measured down to 258 K. Upon further lowering the temperature, we observe a freezing of the translational dynamics while the molecular reorientation is still observable down to 118 K. This suggests that water in the pore center behaves as a plastic amorphous material whose orientational dynamics remains active on a relatively fast (nanoseconds) time scale and feebly temperature dependent, well below what is indicated as water glass transition temperature [12-14]. The consequences of this unexpected observation will be discussed.

## 2. Materials and Methods

The dynamics of water confined in  $\text{AlPO}_4\text{-54}\cdot x\text{H}_2\text{O}$  has been studied by QENS experiments performed at the backscattering spectrometer IN16b at the Institut Laue-Langevin (ILL, Grenoble). Incoherent neutron scattering is a unique probe of individual motions of hydrogen, due to its huge incoherent cross section, typically 2 orders of magnitude larger than in other elements [13-15]. The total coherent and incoherent cross sections for  $\text{AlPO}_4\text{-54}\cdot x\text{H}_2\text{O}$  turn out to be  $\Sigma_{\text{coh}} \approx 484.1$  barn and  $\Sigma_{\text{inch}} \approx 1926.5$  barn. The cross sections of the nanoconfined molecules per unit cell in the fully hydrated sample resulted in  $\Sigma_{\text{coh}} \approx 271.1$  barn and  $\Sigma_{\text{inch}} \approx 5618.2$  barn. Thus the contribution to the total intensity coming from the zeolitic framework is about 29% and is mainly incoherent due to the two  $\text{H}_2\text{O}$  molecules absorbed at the octahedral Al sites. At all temperatures studied, those two water molecules from the  $^{\text{VI}}\text{Al}$  have low atomic displacement parameters (ADP), similar to that for the atoms of  $\text{AlPO}_4$  [1,6], therefore they do not contribute to the measured QENS signal. A polycrystalline  $\text{AlPO}_4\text{-54}\cdot x\text{H}_2\text{O}$  sample (average crystalline dimensions on the order of  $30 \times 1 \times 1 \text{ }\mu\text{m}^3$ ) was

synthesized from nanometric alumina (Pural SB) and phosphoric acid by an optimized sol-gel procedure followed by hydrothermal treatment as described previously [5-8]. 242 mg of powder  $\text{AlPO}_4 \cdot 54 \cdot x\text{H}_2\text{O}$  were loaded into an aluminum sachet to give the sample thickness of  $\sim 2$  mm and mounted on the Displex can.

A fast temperature scan using the Doppler Monochromator in fixed mode at 0  $\mu\text{eV}$  and in accurate velocity mode at 2  $\mu\text{eV}$  was realized to better define the target temperatures for the QENS measurements (see Figure S1 in Supplemental information). Those fast temperature scans show that water dynamics match at best the instrumental time window at about  $T=250$  K. Down to  $T=110$  K some activated dynamics can still be resolved within the energy resolution of the instrument.

The sample was then cooled to the cryostat base temperature at  $T=2$  K and subsequently warmed to 118, 171, 218, 233, 258, 278, 290 and 310 K. The wavelength incident beam has been fixed at 6.271 Å. The energy spectra were recorded at 18 different angles in the range  $10^\circ < 2\theta < 143^\circ$ . Grouping of different angles was performed to obtain sufficiently good statistics. The momentum transfer  $Q$ -range was  $\sim 0.2$ -1.9 Å<sup>-1</sup> and the energy transfer was  $\pm 30$   $\mu\text{eV}$ . A vanadium and the crystalline sample scans were performed at  $T=2$  K to obtain the detector efficiencies and the energy resolution of the instrument, respectively. The resolution function of the spectrometer could be fitted with a Voigt function of FWHM equal to 1.1  $\mu\text{eV}$ .

### 3. Results and Discussion

In Figure 1 we show the measured spectra collected at  $T=258$  K for a selection of momentum transfers  $Q$  from 0.25 Å<sup>-1</sup> to 1.87 Å<sup>-1</sup>, compared to the

instrumental

resolution.

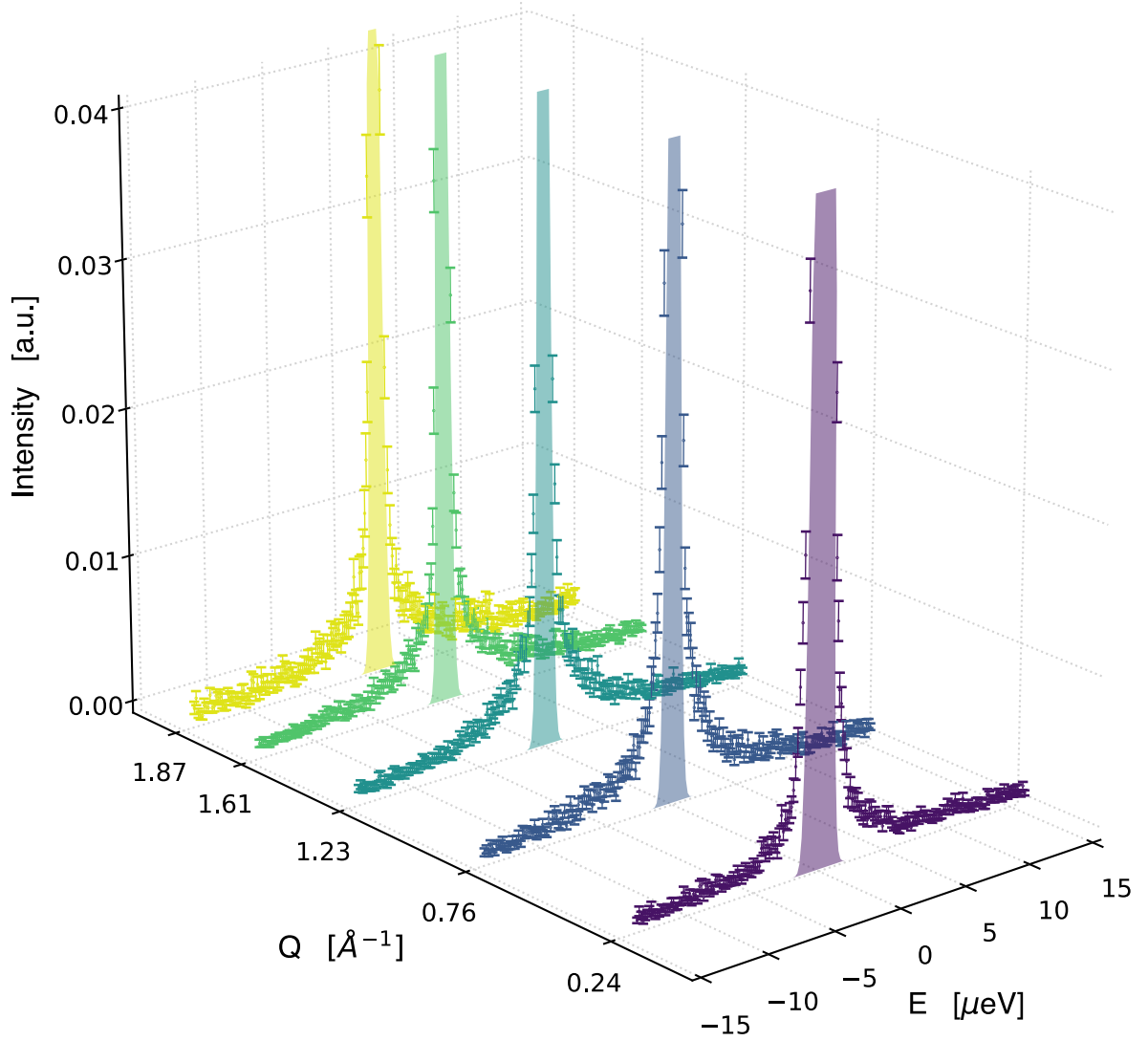


Figure 1: Evolution of the measured QENS intensity of water nanoconfined in  $\text{AlPO}_4\text{-54} \cdot x\text{H}_2\text{O}$  zeolite (dots) at  $T=258$  K for different values of  $Q$  ( $\text{\AA}^{-1}$ ), compared with the experimental resolution (shaded curve).

The measured scattering intensity is proportional to the incoherent scattering function  $S_i(Q, \omega)$  of the unperturbed system, convoluted by the experimental resolution. It can be separated into an elastic and a quasi-elastic contribution. The elastic intensity is here dominated by the immobile (except for vibrations) zeolite frame contributions, while the QENS contribution is due to the confined water diffusing or re-orienting in the zeolite nanopores. As previously



mentioned, the ‘frame’ water bridging Al-octaedra does not contribute to this diffusive motion and thus gives rise to an extra elastic contribution.

In order to extract quantitative information on the timescale and on the nature (diffusive or localized) of the water motions as a function of temperature, we need an analytical expression for the incoherent dynamic structure factor. The latter can be obtained assuming that the vibrational, translational, and rotational motions are decoupled [15-17]. This approximation has been shown to fail in bulk water at low temperatures where water molecule rotation and structural relaxation are strongly entangled [18,19]. However, for water confined in the zeolite, the molecular diffusion timescale is a factor five slower at low temperature than in bulk water [9], while the orientational timescale is similar [9]. As a result the hypothesis of translational-rotational decoupling can be reasonably applied.

The elastic contribution was modelled by a delta function convoluted with the instrumental resolution. In our analysis, we modelled the QENS signal by a single Lorentzian function of HWHM  $\Gamma(Q)$  in the full temperature range. In fact, we considered that for temperatures higher and equal to 258 K, the translational diffusion only can be observed. Above this temperature the rotational diffusion is indeed fast enough to appear as flat background on the energy window of the instrument. The HWHM of the rotational contribution estimated by simulations on zeolite water [9] and data on bulk water [22] is about 40  $\mu\text{eV}$  at 258 K. Conversely, for lower temperatures, the translational diffusion froze - at least on the time resolution of the experiment - while the rotational timescale slows down enough to enter in the instrumental energy window and being measured. In Figure 2 we show an example of fit results compared to the measured intensity for two selected temperatures and selected  $Q$  values. The quality of the fits is

very good and further attempts to model the measured QENS signal with two Lorentzians - associated with the translational and rotational dynamics respectively - in the intermediate temperatures region (233 K, 258 K) did not bring any significant improvement to the fits (Supplemental Figure 2) or change to the measured parameters, which instead become very correlated. Likely the too big temperature step between 233 K and 258 K prevents to observe the regime where both motions contribute to the spectra [15-17].

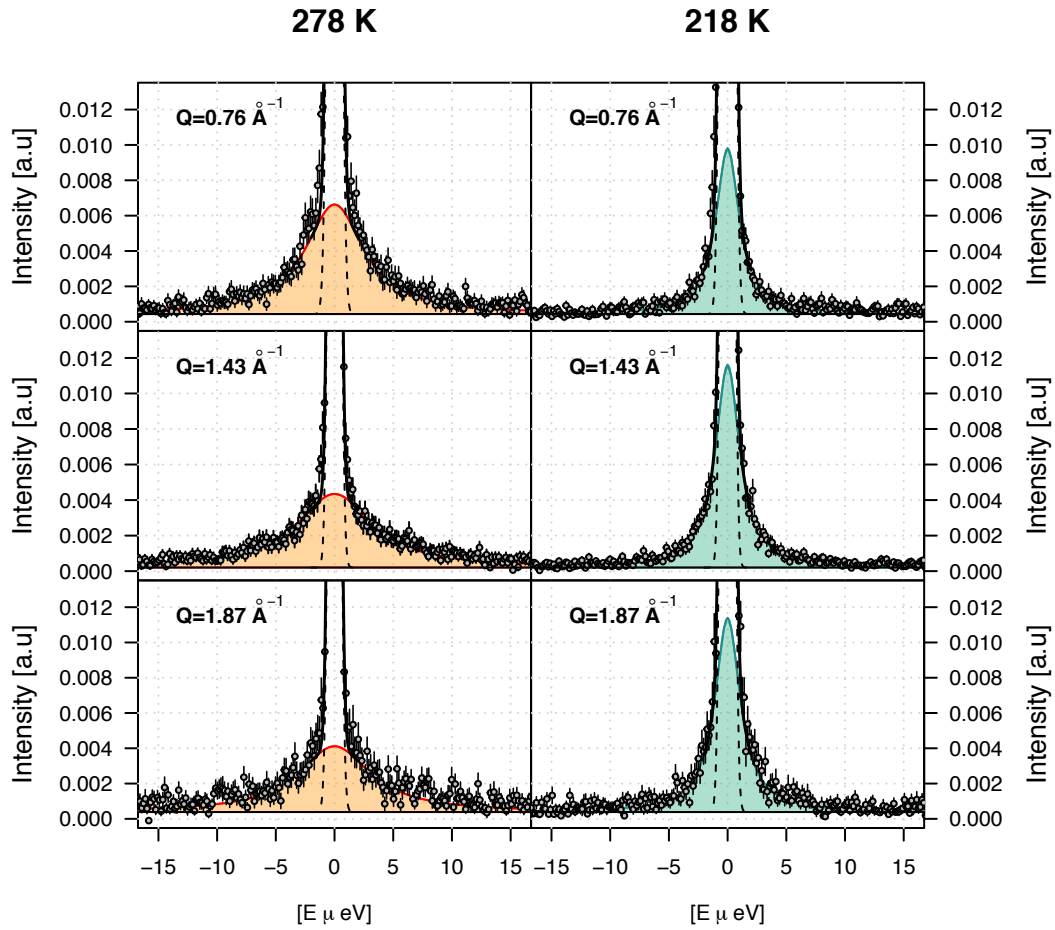


Figure 2: Example of fit results (full black line) compared to the measured intensity (black-grey dots) from water nanoconfined in  $\text{AlPO}_4\text{-54}\cdot x\text{H}_2\text{O}$  zeolite at  $T=278$  K and  $T=218$  K for selected  $Q$  values. The quasi-elastic Lorentzian contribution associated with the translational diffusion at 278 K and with the rotational diffusion at 218 K is shadowed in orange and in green, respectively. The resolution function is shown as a dashed black line.

As shown in Figure 3, we could observe a clear change in the  $Q$  dependence of the  $\Gamma(Q)$  parameter (as well as in the QENS signal intensity reported in

Supplemental Figure 3) associated with the freezing of the translational dynamics and the slowing down of the rotational dynamics. For temperatures higher than or equal to 258 K, the Lorentzian HWHM parameter, here re-named  $\Gamma_T(Q)$  (Figure 3-left panel), shows the typical Q dependence of a jump diffusion process [20], i.e.:

$$\Gamma_T(Q) = D_T Q^2 / (1 + \tau_0 D_T Q^2) \quad (1)$$

where  $\tau_0 = d^2/6D_T$ , with  $D_T$  the mass diffusion coefficient of the confined water molecules and  $d$  representing an apparent jump length [20].

For temperatures lower than or equal to 233 K, the Lorentzian HWHM parameter, here re-named  $\Gamma_R(Q)$  (Figure 3-right panel), shows no Q-dependence within the error bars, as expected for a localized motion. The rotational time scale  $\tau_R = 1/2D_R$  with  $D_R$  the rotational diffusion coefficient has been determined by the fit of  $\Gamma_R(Q) = 2 D_R$  in the full Q range. For the two smaller Q, the intensity of the rotational contribution was too small to allow a proper determination of the width of the QENS signal (see Supplemental Figure 3).

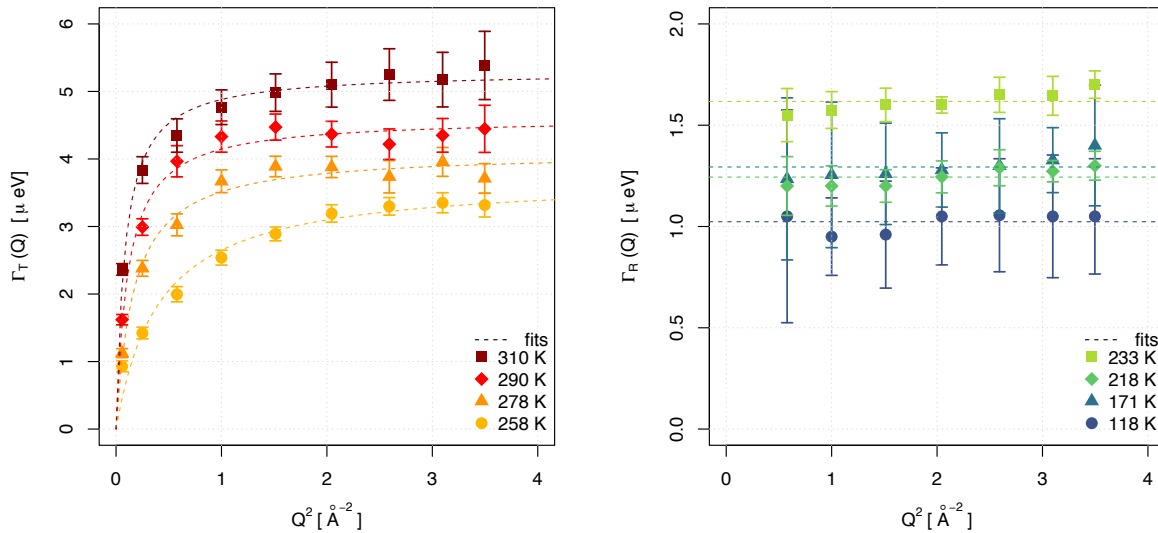


Figure 3: (left panel) HWHM parameter of the Lorentzian function for 310 K, 290 K, 278 K and 258 K, corresponding to a jump diffusion process (dashed line) (right panel) HWHM parameter of the Lorentzian function for 233 K, 218 K, 171 K and 118 K, corresponding to a molecular re-orientation.

The values obtained for  $D_T$  at different temperatures are reported in the left panel of Figure 4, where they are compared to bulk water diffusion coefficients, and in Table 1. At  $T=290$  K, the self-diffusion  $D_T=6.3 \times 10^{-6} \text{ cm}^2/\text{s}$  (Table 1) of nanoconfined water is a factor 4 lower than the one of bulk liquid water ( $1.54 \times 10^{-5} \text{ cm}^2/\text{s}$ ). This value is also in very good agreement with the prediction of molecular dynamics simulations of Barbosa et coworkers [9], who observed translational dynamics being active down to 235 K.

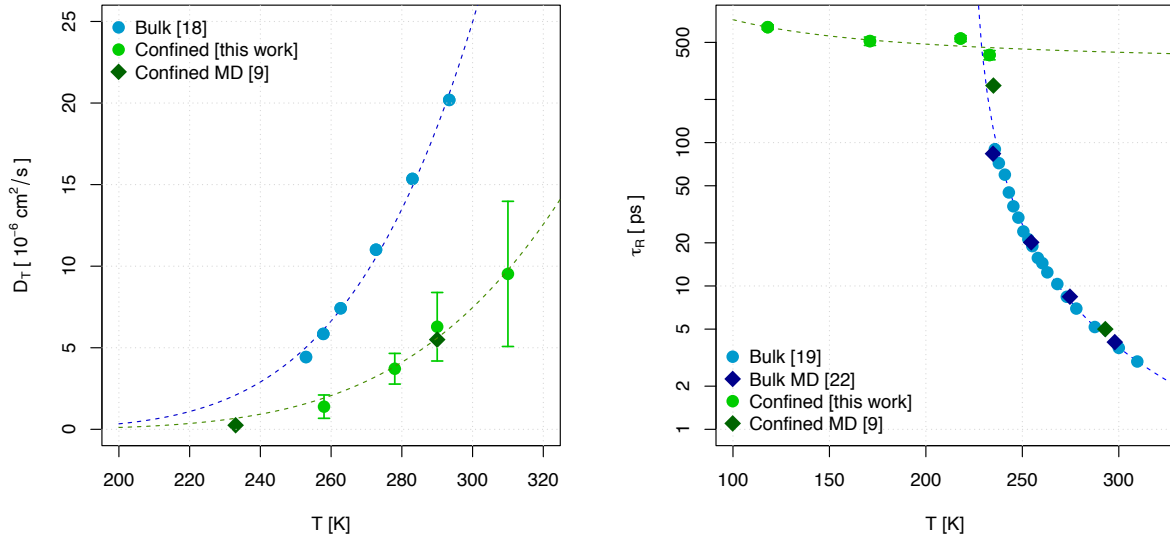


Figure 4: Self-diffusion coefficient (left panel) and molecular rotational time (right panel) of water nanoconfined in  $\text{AlPO}_4\text{-54} \cdot x\text{H}_2\text{O}$  zeolite as a function of temperature measured by QENS (light green dots) compared to simulation results from [9], and to measured [18, 19] and simulated [22] bulk water diffusion. The reorientation time  $\tau_2$  measured by NMR [19] and simulated in [22] for bulk water refers to the molecular dipole re-orientation times. We compared them to the time  $\tau_R=\tau_1=1/2D_R$  [15] measured by QENS under the assumption  $\tau_1 \approx 2\tau_2$ , as predicted by an extended jump model for water rotation [22]. On the left panel, the Arrhenius fits of Eq.2 for bulk and confined water are shown as dashed lines. On the right panel the fit of the  $T > 233$  K bulk water data using expression (3) (in blue) and an Arrhenius fit of confined water for  $T < 233$  K in green are showed.

*Table 1. Mass diffusion and re-orientational time values found for water nanoconfined in  $\text{AlPO}_4\text{-54}\cdot x\text{H}_2\text{O}$  as a function of  $T$ , errors are presented in italic:*

$T$ (K)	$D_T$ ( $\mu\text{eV}\text{\AA}^2$ )	$D_T$ ( $10^{-6}\text{ cm}^2/\text{s}$ )	$\tau_0$ ( $10^{-12}\text{ s}$ )	$T$ (K)	$\tau_R$ ( $10^{-12}\text{ s}$ )
310	62.7 (0.3)	9.5 (4.5)	124 (2)	233	407 (30)
290	41.4 (0.2)	6.3 (2.1)	143 (2)	218	509 (26)
278	24.4 (0.1)	3.7 (0.9)	160 (4)	171	529 (34)
258	9.14 (0.05)	1.4 (0.7)	176 (6)	118	643 (24)

The cage residence time  $\tau_0$  varies with temperature from  $176\pm 6$  ps at the lowest temperature ( $T=258$  K) to  $124 \pm 2$  ps at the higher temperature ( $T=310$  K), corresponding to jump distances of  $d=3.8 \pm 0.3$  Å ( $T=258$  K) and  $d=8.4 \pm 0.5$  Å ( $T=310$  K). The diffusion motion follows an Arrhenius behavior, well described by an activation energy law:

$$D_T(T) = D_0 \exp(-E_a/RT) \quad (2)$$

where  $R=8.314472\text{ JK}^{-1}\text{mol}^{-1}$  is the gas constant.

Using the values obtained for  $D_T$ , the activation energy is roughly estimated to be  $E_a=20.8 \pm 2.8\text{ kJmol}^{-1}$ , with  $D_0=0.031\text{ cm}^2/\text{s}$ . The activation energy  $E_a$  of nanoconfined water in the  $\text{AlPO}_4\text{-54}\cdot x\text{H}_2\text{O}$  zeolite is higher compared to NaX zeolites and bulk water,  $18.7\text{ kJmol}^{-1}$  and  $16.7\text{ kJmol}^{-1}$ , respectively [21].

The values obtained for the re-orientational time,  $\tau_R$ , of zeolite confined water for  $T \leq 233$  K are reported in the right panel of Figure 4 and in Table 1. These values are also compared to the one measured in bulk water [19] and the results of molecular dynamics simulations for bulk [22] and zeolite confined water [9] for the maximum number of inserted water molecules.

The temperature dependence of  $\tau_R$  in bulk water has been described by a singular power law expression [19]:

$$\tau_R(T) = \tau_R^0 (T/T_0 - 1)^{-\gamma} \quad (3)$$

with  $T_0=222.8 \pm 0.4$  K,  $\gamma=1.895 \pm 0.019$  and  $\tau_R^0=0.50 \pm 0.06$  ps.

Eq. 3 is an empirical function that allows to take into account the fact that the apparent activation energy of the re-orientational phenomenon is not constant with temperature but varies due to thermal induced structural changes, changes in viscosity and in dynamical disorder [22].

As we here measure the orientational dynamics for temperatures  $T \leq 233$  K, i.e. once the structural relaxation is frozen and thus no further structural, viscosity, or dynamical disorder changes take place, we observe a recovery of an Arrhenius behaviour  $\tau_R(T) = \tau_0 \exp[E_a / (RT)]$ , with a very feeble temperature activation energy  $E_a = 0.7 \pm 0.2$  kJmol<sup>-1</sup>.

#### 4. Conclusion

The self-dynamics of water molecules nanoconfined in AlPO<sub>4</sub>-54 zeolite were investigated as a function of temperature down to 2 K. High-resolution QENS measurements allowed to measure the molecular diffusion coefficient of confined water down to 258 K. The diffusion is roughly four times slower than diffusion in bulk water and with a slightly higher activation energy. For lower temperatures we measured the water re-orientational dynamics entering the time window of the experiment. This dynamics persists down to 118 K, i.e. well below the hypothetical water glass transition temperature [11] and shows a very feeble temperature dependence. For temperatures lower than 110 K the QENS signal merges into the instrument resolution and no dynamics could be measured.

QENS spectra of water confined in the AlPO<sub>4</sub>-5 zeolite, which possesses smaller unidirectional pores of 7 Å of diameter, were measured at  $T=300$  K by Floquet et al. [23]. The study deduced that, at  $T=300$  K, the water molecular translational mobility was quite small: up to 4H<sub>2</sub>O per unit cell, the diffusion coefficient  $D_T$  was of the order of 10<sup>-6</sup> cm<sup>2</sup>/s, but above this hydration value it

was much smaller than  $10^{-7}$  cm<sup>2</sup>/s. The authors then concluded that the confined water phase in the AlPO<sub>4</sub>-5 nanopore was an “icy” phase already at  $T=300$  K. Therefore the melting temperature of confined water in the AlPO<sub>4</sub>-5 nanopore would be displaced toward the high-temperature side. Conversely, in amorphous silica MCM-41 mesopores, with pore diameter of 24 Å, it was reported to be displaced toward the low temperature side,  $T=230$  K, though more recent investigations have shown that a partial freezing can be already observed at about  $T=240$  K [24,25].

In the present study we observe the freezing of the diffusive dynamics of confined water somewhere between 258 K and 233 K, but the rotational dynamics of water molecules persists well below. The observed rotational dynamics is likely linked to the re-orientation of the inner water molecules, which have been shown [8] to be in a highly disordered and dense amorphous state for temperatures below 240 K. Conversely the molecules in contact with the pore surface are orientationally ordered at low temperatures [8] and are believed not to contribute to the observed dynamics. This observation points to a likely plastic nature of the high density amorphous state of inner water and raise the question if the low temperature “glass” transition observed in calorimetric and dielectric measurements in high density amorphous form of ice (HDA) [26,27] is linked to a similar mechanism.

#### **Corresponding Author**

\*Livia E. Bove, E: [livia.bove@upmc.fr](mailto:livia.bove@upmc.fr) ; T: +33.1.4427.5219 ; Fax: +33.1.4427.3785.

#### **ACKNOWLEDGMENT**

We thank the *Agence Nationale de la Recherche* within the Blanc International programme PACS (reference ANR-13-IS04-0006-01) for financing this study. The quasi-elastic neutron scattering experiments were performed at the IN16b (Experiment proposal 6-7-02 and experiment LTP-6-6), in the Institut Laue-Langevin (ILL).

#### Author contributions

The project was conceived by F.G.A and L.E.B., the experiments were performed by F.G.A., U.R, B.F. and L.E.B. The data were analyzed by M.L., M.R and L.E.B. The figures were produced by M.R., with inputs from L.E.B.. The manuscript was written by L.E.B. All authors discussed the results and commented on the manuscript.

#### References

- [1] W.M. Meier, D.H. Olson, Atlas of zeolite structure types, 3rd rev. ed, Published on behalf of the Structure Commission of the International Zeolite Association by Butterworth-Heinemann, London ; Boston, 1992.
- [2] C.J. Rhodes, Properties and applications of Zeolites, Science Progress. 93 (2010) 223–284. <https://doi.org/10.3184/003685010X12800828155007>.
- [3] Y. Li, J. Yu, Emerging applications of zeolites in catalysis, separation and host-guest assembly, Nat Rev Mater. 6 (2021) 1156–1174. <https://doi.org/10.1038/s41578-021-00347-3>.
- [4] T.A. Aragaw, A.A. Ayalew, Removal of water hardness using zeolite synthesized from Ethiopian kaolin by hydrothermal method, Water Practice and Technology. 14 (2019) 145–159. <https://doi.org/10.2166/wpt.2018.116>.
- [5] F.G. Alabarse, J. Haines, O. Cambon, C. Levelut, D. Bourgogne, A. Haidoux, D. Granier, B. Coasne, Freezing of Water Confined at the Nanoscale, Phys. Rev. Lett. 109 (2012) 035701. <https://doi.org/10.1103/PhysRevLett.109.035701>.
- [6] F.G. Alabarse, J. Rouquette, B. Coasne, A. Haidoux, C. Paulmann, O. Cambon, J. Haines, Mechanism of H<sub>2</sub>O Insertion and Chemical Bond Formation in AlPO<sub>4</sub>-54·xH<sub>2</sub>O at High Pressure, J. Am. Chem. Soc. 137 (2015) 584–587. <https://doi.org/10.1021/ja511153n>.
- [7] F.G. Alabarse, G. Silly, A. Haidoux, C. Levelut, D. Bourgogne, A.-M. Flank, P.



- Lagarde, A.S. Pereira, J.-L. Bantignies, O. Cambon, J. Haines, Effect of H<sub>2</sub>O on the Pressure-Induced Amorphization of AlPO<sub>4</sub>-54·x H<sub>2</sub>O, *J. Phys. Chem. C*. 118 (2014) 3651–3663. <https://doi.org/10.1021/jp412181f>.
- [8] F.G. Alabarse, B. Baptiste, M. Jiménez-Ruiz, B. Coasne, J. Haines, J.-B. Brubach, P. Roy, H.E. Fischer, S. Klotz, L.E. Bove, Different Water Networks Confined in Unidirectional Hydrophilic Nanopores and Transitions with Temperature, *J. Phys. Chem. C*. 125 (2021) 14378–14393. <https://doi.org/10.1021/acs.jpcc.1c01254>.
- [9] C. Gavazzoni, N. Giovambattista, P.A. Netz, M.C. Barbosa, Structure and mobility of water confined in AlPO<sub>4</sub>-54 nanotubes, *The Journal of Chemical Physics*. 146 (2017) 234509. <https://doi.org/10.1063/1.4985626>.
- [10] M. Majumder, N. Chopra, R. Andrews, B.J. Hinds, Enhanced flow in carbon nanotubes, *Nature*. 438 (2005) 44–44. <https://doi.org/10.1038/438044a>.
- [11] J.K. Holt, H.G. Park, Y. Wang, M. Stadermann, A.B. Artyukhin, C.P. Grigoropoulos, A. Noy, O. Bakajin, Fast Mass Transport Through Sub-2-Nanometer Carbon Nanotubes, *Science*. 312 (2006) 1034–1037. <https://doi.org/10.1126/science.1126298>.
- [12] G.P. Johari, A. Hallbrucker, E. Mayer, The glass–liquid transition of hyperquenched water, *Nature*. 330 (1987) 552–553. <https://doi.org/10.1038/330552a0>.
- [13] C.A. Angell, Insights into Phases of Liquid Water from Study of Its Unusual Glass-Forming Properties, *Science*. 319 (2008) 582–587. <https://doi.org/10.1126/science.1131939>.
- [14] P. Lucas, J. Pries, S. Wei, M. Wuttig, The glass transition of water, insight from phase change materials, *Journal of Non-Crystalline Solids: X*. 14 (2022) 100084. <https://doi.org/10.1016/j.nocx.2022.100084>.
- [15] L.E. Bove, S. Klotz, Th. Strässle, M. Koza, J. Teixeira, A.M. Saitta, Translational and Rotational Diffusion in Water in the Gigapascal Range, *Phys. Rev. Lett.* 111 (2013) 185901. <https://doi.org/10.1103/PhysRevLett.111.185901>.
- [16] K. Amann-Winkel, M.-C. Bellissent-Funel, L.E. Bove, T. Loerting, A. Nilsson, A. Paciaroni, D. Schlesinger, L. Skinner, X-ray and Neutron Scattering of Water, *Chem. Rev.* 116 (2016) 7570–7589. <https://doi.org/10.1021/acs.chemrev.5b00663>.
- [17] U. Ranieri, P. Giura, F.A. Gorelli, M. Santoro, S. Klotz, P. Gillet, L. Paolasini, M.M. Koza, L.E. Bove, Dynamical Crossover in Hot Dense Water: The Hydrogen Bond Role, *J. Phys. Chem. B*. 120 (2016) 9051–9059. <https://doi.org/10.1021/acs.jpcb.6b04142>.
- [18] J. Qvist, H. Schober, B. Halle, Structural dynamics of supercooled water from

quasielastic neutron scattering and molecular simulations, *J. Chem. Phys.* 134 (2011) 144508. <https://doi.org/10.1063/1.3578472>.

[19] J. Qvist, C. Mattea, E.P. Sunde, B. Halle, Rotational dynamics in supercooled water from nuclear spin relaxation and molecular simulations, *J. Chem. Phys.* 136 (2012) 204505. <https://doi.org/10.1063/1.4720941>.

[20] K.S. Singwi, A. Sjölander, Diffusive Motions in Water and Cold Neutron Scattering, *Phys. Rev.* 119 (1960) 863–871. <https://doi.org/10.1103/PhysRev.119.863>.

[21] F. González Sánchez, F. Jurányi, T. Gimmi, L. Van Loon, T. Unruh, L.W. Diamond, Translational diffusion of water and its dependence on temperature in charged and uncharged clays: A neutron scattering study, *J. Chem. Phys.* 129 (2008) 174706. <https://doi.org/10.1063/1.3000638>.

[22] G. Stirnemann, D. Laage, Communication: On the origin of the non-Arrhenius behavior in water reorientation dynamics, *J. Chem. Phys.* 137 (2012) 031101. <https://doi.org/10.1063/1.4737390>.

[23] N. Floquet, J.P. Coulomb, N. Dufau, G. Andre, R. Kahn, Confined Water in Mesoporous MCM-41 and Nanoporous AlPO<sub>4</sub>-5: Structure and Dynamics, *Adsorption*. 11 (2005) 139–144. <https://doi.org/10.1007/s10450-005-5912-9>.

[24] E. Stefanutti, L.E. Bove, G. Lelong, M.A. Ricci, A.K. Soper, F. Bruni, Ice crystallization observed in highly supercooled confined water, *Phys. Chem. Chem. Phys.* 21 (2019) 4931–4938. <https://doi.org/10.1039/C8CP07585A>.

[25] E. Stefanutti, L.E. Bove, F.G. Alabarse, G. Lelong, F. Bruni, M.A. Ricci, Vibrational dynamics of confined supercooled water, *J. Chem. Phys.* 150 (2019) 224504. <https://doi.org/10.1063/1.5094147>.

[26] O. Andersson, Relaxation Time of Water's High-Density Amorphous Ice Phase, *Phys. Rev. Lett.* 95 (2005) 205503. <https://doi.org/10.1103/PhysRevLett.95.205503>.

[27] K. Amann-Winkel, C. Gainaru, P.H. Handle, M. Seidl, H. Nelson, R. Böhmer, T. Loerting, Water's second glass transition, *Proc. Natl. Acad. Sci. U.S.A.* 110 (2013) 17720–17725. <https://doi.org/10.1073/pnas.1311718110>.

## Supplemental

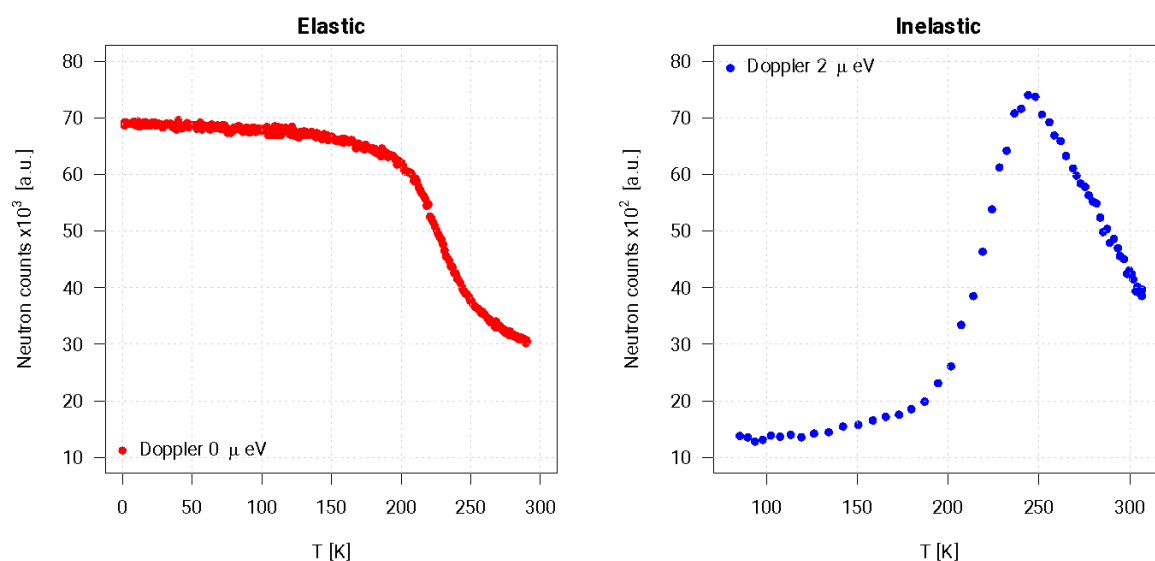


Figure 1S: Intensity of neutron counts at Doppler 0  $\mu$ eV (*Left*) and at 2  $\mu$ eV (*Right*), respectively elastic and inelastic, as function of  $T$  in  $\text{AlPO}_4\cdot 54\cdot x\text{H}_2\text{O}$ .

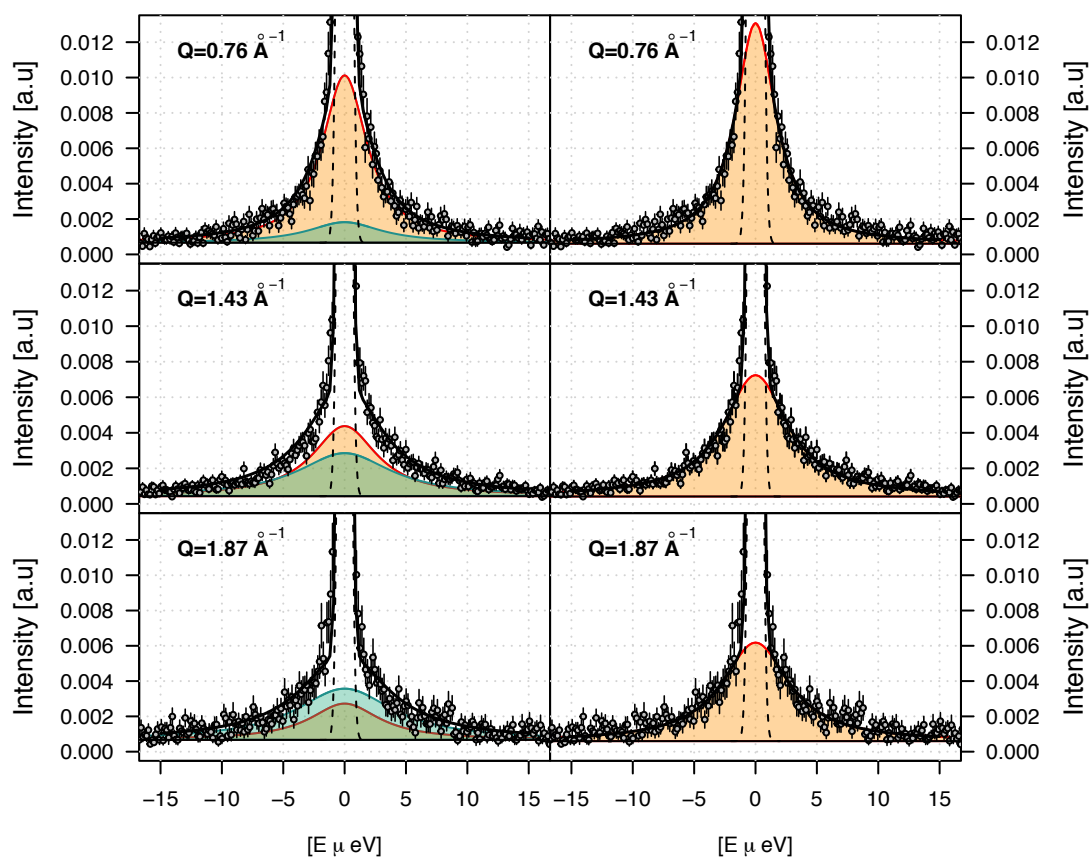


Figure 2S: Example of fit results of the QENS signal with two Lorentzian functions at  $T=258 \text{ K}$  for three selected  $Q$  values. Fits with only one Lorentzian contribution are shown for comparison.

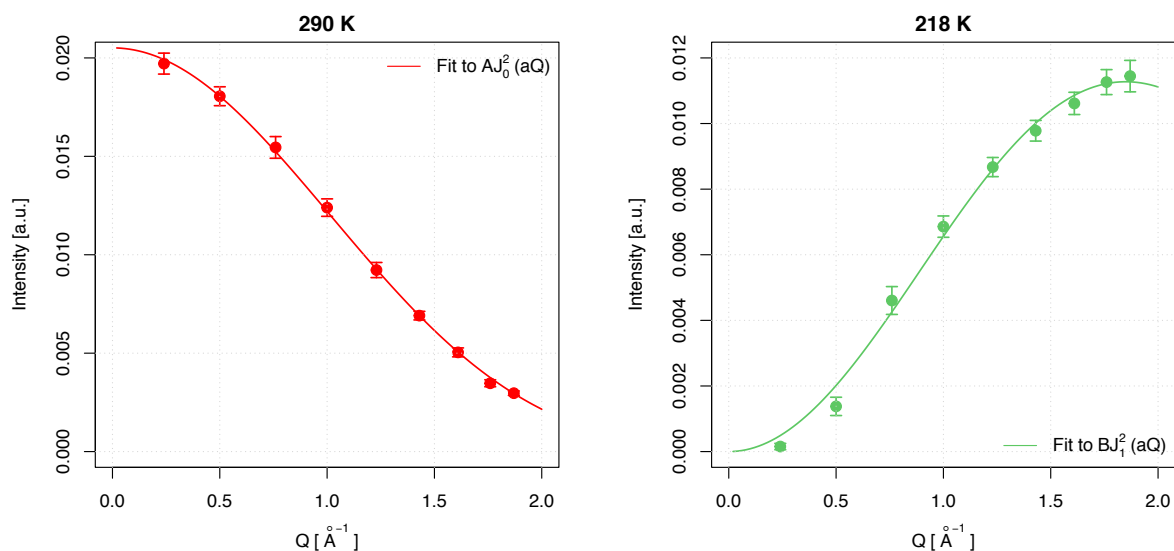


Figure 3S: Intensity of the quasi-elastic translational (left) and rotational (right) signals as a function of  $Q$  at  $T=290$  K and  $218$  K, respectively. The intensity of the translational term is proportional to a Bessel function of 0 order as  $j_0^2(aQ)$ , while the rotational diffusion term is proportional to a Bessel function of 1st order  $j_1^2(aQ)$ , with  $a=0.98 \text{ \AA}$  fixed to the radius of the water molecule.